Linear Stability of Finite-Difference Approximations on a Uniform Latitude-Longitude Grid with Fourier Filtering

DAVID L. WILLIAMSON

National Center for Atmospheric Research,[1] Boulder, Colo. 80303

(Manuscript received 11 June 1975, in revised form 22 August 1975)

ABSTRACT

The linear stability condition for explicit, second-order, centered difference approximations to the shallow-water equations on a uniform latitude-longitude spherical grid is determined. The grid has points at the poles and on the equator. Two modifications involving Fourier filtering in the longitudinal direction are considered to permit a longer stable time step. In the first, the prognostic variables are filtered, while in the second the zonal pressure gradient in the zonal momentum equation and the zonal divergence in the continuity equation are filtered. Both modifications permit approximately the same time step when the wavenumber cutoff is the same. Although filtering can be performed at all latitudes, the most efficient procedure involves filtering only near the poles. To allow a reasonable time step, all but approximately the six longest waves must be removed at the first row of points next to the pole. This filtering next to the pole determines a time step such that additional filtering is necessary at only a few latitudes, usually poleward of 80°.

The stability condition is also found for second- and fourth-order approximations on a shifted mesh in which the first grid points are a half-grid interval away from the pole. Only filtering of the prognostic variables is considered. As in the previous case, to allow a reasonable time step, only the longest waves can be retained next to the pole. This filtering determines a time step such that filtering is not required at all latitudes. When such filtering is performed, the second- and fourth-order schemes have approximately the same stable time step. The modifications to the free oscillations of the model caused by the filtering are also discussed.

1. Introduction

In the past, much effort has been devoted to developing spherical grids with uniform distance between grid points. Such grids were desired because of the excessively small time step that would be required by linear stability for an explicit difference scheme applied to a grid uniform in latitude and longitude. Kurihara (1965) developed a grid with points on uniformly spaced latitude circles, but with the longitudinal grid increment increasing with increasing latitude such that the distance between grid points was nearly constant. Kurihara and Holloway (1967) integrated a nine-level primitive equation model on this grid using finite differences based on the box method. Kasahara and Washington (1967, 1971) and Washington and Kasahara (1970) developed a baroclinic global circulation model over a grid uniform in latitude and longitude equatorward of some critical latitude (70° in the first version, then decreased to 60° in later versions). Poleward of this critical latitude, grid points were dropped in the longitudinal direction so that the distance between grid points did not continue to decrease approaching the poles. Their model used centered differences with the values needed by the latitudinal differences supplied by linear interpolation in the longitudinal direction.

Dey (1969) examined the truncation error in computing cross-polar flow on the Kurihara grid. He found that the scheme produced spurious polar anticyclogenesis for this flow. The error was reduced to acceptable levels by providing more resolution at high latitudes. However, a smaller time step was required by this increased polar resolution. A similar study by Sankar-Rao and Umscheid (1969) produced similar results.

Umscheid and Sankar-Rao (1971) tested two smoothing techniques as a practical means of allowing a larger time step with the modified Kurihara grid. In one method, they filtered the zonal mass flux in the divergence equation and the zonal pressure gradient in the zonal momentum equation using Fourier expansions, so that these fields consisted only of wavelengths greater than the latitudinal grid increment. In the following, we consider only Fourier filtering and not other grid point filters such as those also considered by Umscheid and Sankar-Rao (1971) and Vanderman (1972).

Holloway *et al.* (1973) and Williamson and Browning (1973) considered the use of a uniform latitude-longitude grid coupled with Fourier filtering to allow a reasonable time step. In both studies, all prognostic

[1] The National Center for Atmospheric Research is sponsored by the National Science Foundation.

variables were filtered at each time step poleward of some critical latitude so that the minimum wavelength at any latitude was greater than the minimum wavelength at the critical latitude. Holloway *et al.* took this critical latitude to be 45° while Williamson and Browning used 60°. In an appendix, Holloway *et al.* (1973) included a stability analysis for the difference equations coupled with the Fourier filtering; however, the analysis was based on one-dimensional cartesian geometry and does not carry over directly to the spherical geometry.

In the following, we determine the minimum filtering needed for computational stability given the grid resolution and time step desired for integrating over a latitude-longitude grid. To do so, the linear stability of centered difference approximations on a uniform latitude-longitude grid with and without Fourier filtering is determined. The analysis is performed for the shallow-water equations. Baroclinic models linearized around relatively simple mean states can be reduced to a series of shallow-water equations by separation of variables. An example is given in Williamson and Dickinson (1976) for the NCAR Global Circulation Model. For the stability analysis, we follow the normal mode analysis of Dickinson and Williamson (1972), hereafter referred to as D&W.

2. Stability analysis

The centered difference approximations to the shallow-water equations linearized about a state of rest are

$$\left.\begin{aligned} \delta_t u_{ij}^\tau - f v_{ij}^\tau + \frac{g}{a\cos\varphi_j}\delta_\lambda h_{ij}^\tau = 0 \\ \delta_t v_{ij}^\tau + f u_{ij}^\tau + \frac{g}{a}\delta_\varphi h_{ij}^\tau = 0 \\ \delta_t h_{ij}^\tau + \frac{D}{a\cos\varphi_j}[\delta_\lambda u_{ij}^\tau + \delta_\varphi(v_{ij}^\tau \cos\varphi_j)] = 0 \end{aligned}\right\}, \quad (2.1)$$

where u, v, and h are the grid point values of the zonal wind, meridional wind and height, g is gravity, a the radius of the earth, λ longitude, φ latitude, t time, D the mean depth of the fluid and f the Coriolis parameter. The discrete difference operators are given by

$$\left.\begin{aligned} \delta_t \psi_{ij}^\tau &= \frac{\psi_{ij}^{\tau+1} - \psi_{ij}^{\tau-1}}{2\Delta t} \\ \delta_\lambda \psi_{ij}^\tau &= \frac{\psi_{i+1,j}^\tau - \psi_{i-1,j}^\tau}{2\Delta\lambda} \\ \delta_\varphi \psi_{ij}^\tau &= \frac{\psi_{i,j+1}^\tau - \psi_{i,j-1}^\tau}{2\Delta\varphi} \end{aligned}\right\}. \quad (2.2)$$

The grid points are defined as intersections of equally spaced circles of constant latitude and longitude with grid points at the poles and on the equator. The longitude, latitude and temporal indices are i, j and τ, respectively. Only height is needed at the poles and it is determined by computing the mass flux into the polar caps. The velocities are not needed at the poles in the finite-difference equations.

We separate time and longitude variables by assuming

$$\begin{bmatrix} u \\ v \\ h \end{bmatrix}_{ij}^\tau = \begin{bmatrix} u \\ v \\ h \end{bmatrix}_{kj}^\nu e^{i(k\lambda+\nu t)}. \quad (2.3)$$

Substitution of (2.3) into (2.1) yields

$$\left.\begin{aligned} i\nu' u_j - f_j v_j + \frac{igk'}{a\cos\varphi_j} h_j = 0 \\ i\nu' v_j + f_j u_j + \frac{g}{a}\frac{h_{j+1}-h_{j-1}}{2\Delta\varphi} = 0 \\ i\nu' h_j + \frac{D}{a\cos\varphi_j} \times \left(ik' u_j + \frac{v_{j+1}\cos\varphi_{j+1} - v_{j-1}\cos\varphi_{j-1}}{2\Delta\varphi}\right) = 0 \end{aligned}\right\}, \quad (2.4)$$

where

$$\nu' = \frac{\sin\nu\Delta t}{\Delta t} \quad (2.5)$$

and

$$k' = \frac{\sin k\Delta\lambda}{\Delta\lambda}. \quad (2.6)$$

In (2.4), subscript k and superscript ν have been dropped. Equations (2.4) apply at every latitude and represent a coupled system of equations for coefficients u_j, v_j and h_j at each latitude.

D&W show how system (2.4) can be transformed to an eigenvalue problem of the form

$$\mathbf{L}\mathbf{Y} + \nu'\mathbf{Q}\mathbf{Y} = 0, \quad (2.7)$$

where the eigenvector $\mathbf{Y}$ is proportional to the vector formed from the unknowns u_j, v_j and h_j. The matrices $\mathbf{L}$ and $\mathbf{Q}$ contain the parameters in the equations such as f_j, $\cos\varphi_j$, a, k' etc. The eigenvalue ν' is related to the frequency of oscillation ν of the solutions of (2.3) by (2.5). Details of the matrices, transformations involved, and method of solution are given in D&W and not repeated here. It is also shown in D&W that for the problem considered here the eigenvalues ν' are real and come in pairs with the same magnitude but opposite sign. The maximum stable time step is then determined by requiring that every ν be real. The frequency of oscillation ν is obtained by inverting

(2.5) giving

$$\nu=[\arcsin(\nu'\Delta t)]/\Delta t, \tag{2.8}$$

which, in turn, requires that for the scheme to be linearly stable

$$\Delta t\leq\frac{1}{|\nu'|} \tag{2.9}$$

for all ν'.

Eq. (2.9) represents the linear stability condition for the particular discrete forecast model considered. As will be seen later, Δt is relatively small when the discrete equations are applied to the uniform latitude-longitude grid.

Two modifications to the scheme above are considered. For the first, the short longitudinal waves are removed near the poles every time step by Fourier filtering the prognostic variables u, v and h. In the second, the zonal pressure gradient term in the u-equation and the zonal divergence term in the h-equation are filtered every time step near the poles.

In the first method, the Fourier amplitudes of the prognostic variables are set to zero every time step at polar latitudes for wavenumbers greater than some cutoff wavenumber. This filtering has the effect in the eigenvalue problem (2.7) of setting the components of the vectors $\mathbf{Y}$, i.e., the scalars u_j, v_j and h_j, equal to zero for these wavenumbers and latitudes. The matrix problem retains the same form (2.7), but the last components of the vector $\mathbf{Y}$ and the matrices $\mathbf{L}$ and $\mathbf{Q}$ have subscripts $-N+Z$ and $N-Z$ rather than $-N+1$ and $N-1$, respectively, where Z is the number of latitudinal grid points in each hemisphere (including the pole) at which the vectors are assumed zero [see Eq. (3.29) in D&W for the form of $\mathbf{L}$]. We assume that the same filtering is performed in each hemisphere.

In the case without filtering, the order of the matrix $\mathbf{L}$ is $3(N-2)$ for the global problem, where N is the number of latitudinal grid points (including the poles). For this case, there are $3(N-2)$ eigenvectors for each longitudinal wavenumber k. When the filtering is performed, the order of $\mathbf{L}$ is $3(N-2Z)$. Thus, six eigenvectors are eliminated for each latitude where filtering is performed.

In the second method, only the pressure gradient and divergence terms are filtered. No assumption is made concerning the structure of the eigenvectors $\mathbf{Y}$ near the poles. In this case, the eigenvalue problem (2.7) is of the same order as when no filtering is performed. The only difference is in the block matrices $\mathbf{A}_j$ in the definition of $\mathbf{L}$. [The definition of $\mathbf{A}$ for the problem including a mean wind is given by Eq. (3.23) in D&W and not repeated here.] At the latitudes at which no filtering is performed, $\mathbf{A}_j$ is defined by (3.23) in D&W with the mean wind set to zero. However, at those latitudes where filtering is performed, $\mathbf{A}_j$ becomes

$$\mathbf{A}_j=\begin{bmatrix}0 & -\sigma_j f_j & 0\\ -\sigma_j f_j & 0 & 0\\ 0 & 0 & 0\end{bmatrix}. \tag{2.10}$$

3. Solutions

We now consider the effect of the polar filtering on the actual eigenvalues and eigenvectors. We first briefly review the nature of the solutions of the eigenvalue problem (2.7); a more thorough description is given in D&W. For fixed longitudinal wavenumber k, the low-index, large meridional-scale modes of the difference equations (2.1) correspond closely to the modes of the differential equations and are classified accordingly as Rossby and Eastward and Westward gravity modes. The remaining modes are classified as Rossby modes if their frequencies are no larger in magnitude than the frequency of the lowest-index Rossby modes. Likewise, these remaining modes are classified as gravity modes if their frequencies are no smaller in magnitude than the frequency of the lowest-index gravity modes. In general, the eigenvalues ν' come in pairs with equal magnitude and opposite sign. One of the pair corresponds to a solution of the continuous equations and is referred to as a "good" mode. The other generally has a $2\Delta\varphi$ structure modulated by a larger-scale wave and is referred to as a "computational" mode. The distinction between "good" and "computational" Rossby modes is not clear when considering the structure of the smaller-scale modes. The high-index "good" modes have a $4\Delta\varphi$ scale and, therefore, a rather choppy appearance on the discrete grid unlike the corresponding solutions of the continuous equations. Also, their frequencies tend to differ more from the continuous case than do the lower-index modes.

Table 1 lists the eigenvalues ν' for $D=10^4$ m and $k=7$ for the Rossby and Westward gravity modes on a 5° grid for the case of no filtering, filtering u, v and h at 85°, and filtering $\delta_\lambda h$ and $\delta_\lambda u$ at 85°. The table lists slightly more than half the eigenvalues in each case; thus, the frequencies of some computational modes are included in the table. The computational modes are those with the latitudinal index l greater than 17 in columns 1 and 3, greater than 16 in columns 2, 4 and 6, and greater than 15 in column 5. The computational Rossby modes have a sign opposite to the good Rossby modes. We compare first the no-filtering case with the case filtering h, u and v. The low-index modes are virtually unchanged by filtering. The eigenvalues of the first 12 Rossby modes and the first 15 Westward gravity modes are identical to 4 digits. The horizontal lines in the table indicate the end of the good modes. There are two fewer modes in each category when the prognostic variables are filtered at 85°, one computational mode and one good mode. The $l=17$ and 18 Rossby modes and the $l=16$

TABLE 1. Eigenvalue ν' for $k=7$ and $D=10^4$ m with a 5° grid.

l	No filtering	Rossby h, u, & v filtered at 85°	$\delta_\lambda h$ & $\delta_\lambda u$ filtered at 85°	No filtering	Westward gravity h, u, & v filtered at 85°	$\delta_\lambda h$ & $\delta_\lambda u$ filtered at 85°
0	1.887E-5	1.887E-5	1.887E-5	3.579E-4	3.579E-4	3.579E-4
1	1.391E-5	1.391E-5	1.391E-5	4.056E-4	4.056E-4	4.056E-4
2	1.065E-5	1.065E-5	1.065E-5	4.508E-4	4.508E-4	4.508E-4
3	8.365E-6	8.365E-6	8.365E-6	4.935E-4	4.935E-4	4.935E-4
4	6.676E-6	6.676E-6	6.676E-6	5.332E-4	5.332E-4	5.332E-4
5	5.383E-6	5.383E-6	5.383E-6	5.695E-4	5.695E-4	5.695E-4
6	4.365E-6	4.365E-6	4.365E-6	6.017E-4	6.017E-4	6.017E-4
7	3.544E-6	3.544E-6	3.543E-6	6.287E-4	6.287E-4	6.287E-4
8	2.869E-6	2.869E-6	2.867E-6	6.526E-4	6.526E-4	6.526E-4
9	2.302E-6	2.302E-6	2.297E-6	6.811E-4	6.811E-4	6.811E-4
10	1.821E-6	1.821E-6	1.809E-6	7.222E-4	7.222E-4	7.222E-4
11	1.407E-6	1.407E-6	1.383E-6	7.845E-4	7.845E-4	7.845E-4
12	1.051E-6	1.049E-6	1.002E-6	8.813E-4	8.813E-4	8.813E-4
13	7.433E-7	7.382E-7	6.525E-7	1.039E-3	1.039E-3	1.039E-3
14	4.824E-7	4.668E-7	3.218E-7	1.320E-3	1.320E-3	1.322E-3
15	2.687E-7	2.252E-7	0	1.908E-3	1.898E-3	1.909E-3
16	1.091E-7	0	1.444E-4	3.731E-3	1.898E-3	3.898E-4
17	0	−2.252E-7	1.444E-4	3.731E-3	1.320E-3	3.898E-4
18	−1.091E-7	−4.668E-7	−1.444E-4	1.908E-3	1.039E-3	1.909E-3
19	−2.687E-7	−7.382E-7	−1.444E-4	1.320E-3	8.813E-4	1.322E-3
20	−4.824E-7	−1.049E-6	−3.218E-7	1.039E-3	7.845E-4	1.039E-3

and 17 Westward gravity modes of the no-filtering case are not present in the filtering case. Although the filtering eliminates "good" Rossby modes, the eliminated modes are the highest-index ones which differ most from the corresponding solutions to the continuous equation, as discussed earlier, and there is little harm in eliminating them.

The changes in frequencies of the Rossby modes are somewhat greater when $\delta_\lambda h$ and $\delta_\lambda u$ are filtered rather than h, u and v. Although the number of modes is the same when filtering $\delta_\lambda h$ and $\delta_\lambda u$ as with no filtering, some modes are drastically changed. These appear between the horizontal lines and do not correspond to the modes from the other methods. Essentially, frequencies of the fastest gravity waves and slowest Rossby waves of the no-filtering case are changed such that they fall in magnitude between the Rossby and gravity waves. As will be seen, the shapes of the modes are changed as well. The modified Rossby modes are those for which it is difficult to distinguish "good" and "computational" (as discussed earlier). They have a $4\Delta\varphi$ structure and thus represent the continuous modes poorly. These modified modes do not correspond to the solutions of the continuous equations and do not fit into the categories defined in D&W.

Figure 1 shows the height field h vs latitude of the $l=6$, 15, 16 and 17 Rossby modes for these three cases. These modes are normalized so that the inner product $\sum_j \sigma_j \mathbf{Y}_j \cdot \mathbf{Y}_j$ is unity. The S or A in the figure indicates if the height is symmetric or antisymmetric with respect to the equator. The $l=6$ mode is identical in all three cases. This mode is almost zero at 85° in the no-filtering case, so there is no change when it is filtered at 85°. The feature is common to all low-index modes except for the smallest longitudinal wavenumbers for which the maximum frequency is so small that filtering is not necessary. The $l=15$ and 16 modes show a slight change from no-filtering to filtering u, v, and h at 85°. The change can be interpreted as a slight equatorward compression of the wave structure. The $l=17$ mode in the no-filtering case is lost when u, v, and h are filtered at 85°.

The $l=15$ mode shows even more equatorward compression of the structure when $\delta_\lambda u$ and $\delta_\lambda h$ are filtered at 85° than when u, v, and h are. Even though the vectors are not forced to be zero at 85°, the solutions turn out to be close to zero at 80° and 85°. The $l=16$ and 17 modes from filtering $\delta_\lambda u$ and $\delta_\lambda h$ at 85° do not correspond to those shown with no filtering. These are two modes resulting from the filtering that have relatively low frequencies, but do not correspond to solutions of the continuous equations or to modes from the no-filtering case.

Figure 2 shows the height field of the $l=6$, 14, 15 and 16 Westward gravity waves for the same cases as Fig. 1. As with the Rossby mode, there is no change in the low-order gravity modes from filtering as evi-

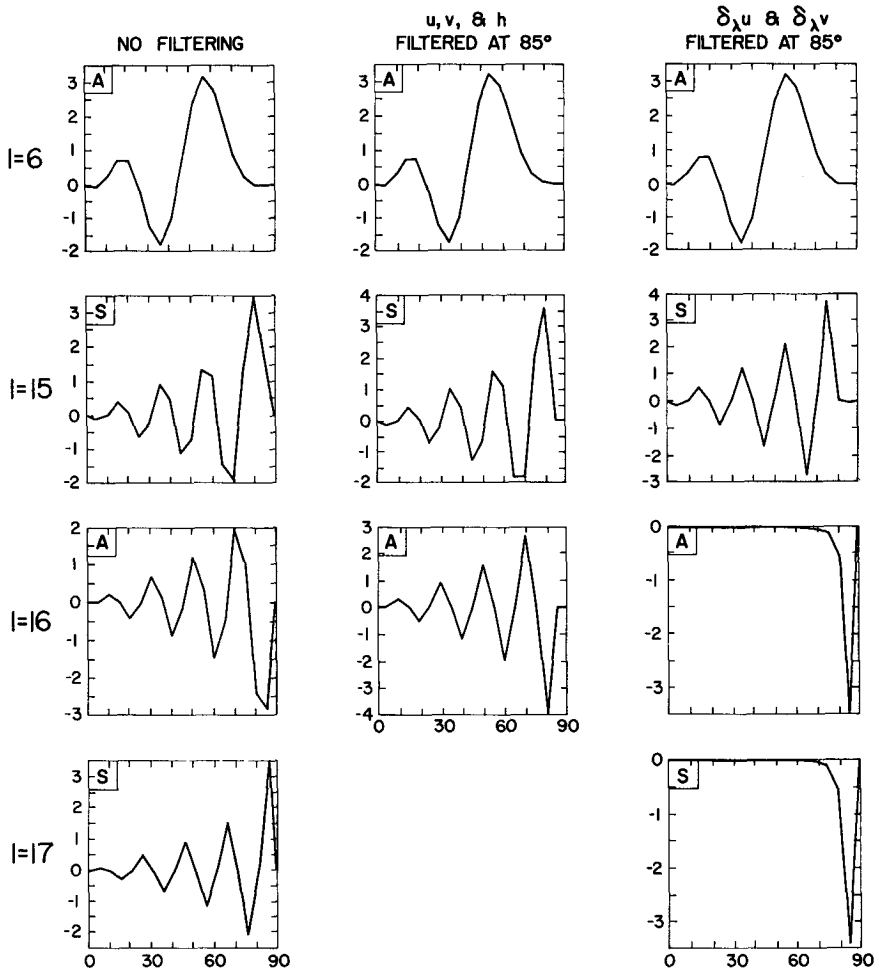

FIG. 1. Height as a function of latitude for the $k=7$ Rossby modes with $D=10^4$ m for latitude indices 6, 15, 16, and 17. S indicates that the height is symmetric with respect to the equator and A antisymmetric.

dent by the $l=6$ mode. Even the $l=14$, and 15 modes show only small differences, and then only at 85°. The $l=16$ mode is essentially just a blip at 85°. This mode is eliminated by filtering u, v, and h at 85°, while the frequency is greatly decreased by filtering $\delta_\lambda u$ and $\delta_\lambda h$ with little change in the structure of the mode in this case.

Filtering at latitudes lower than 85° has an effect similar to filtering at 85°. The main differences are that more modes are eliminated by filtering u, v, and h, and more modes have the large frequency shifts and structure changes when filtering $\delta_\lambda u$ and $\delta_\lambda h$. The differences caused by the filtering procedures in the modes that are not eliminated or drastically modified are even less for smaller equivalent depths D. As illustrated in D&W, the same-index mode is concentrated more toward the equator when the equivalent depth is smaller. Thus, the artificial constraint that they be zero at some latitude other than the pole has less effect on these modes.

4. Maximum stable time steps

The maximum stable Δt can be determined from the largest frequency for each longitudinal wavenumber k. Table 1 for $k=7$ shows that this value is the frequency of the highest-index "good" gravity mode. These high-index "good" Eastward and Westward gravity modes have frequencies with the same magnitude. For the case of no filtering, the maximum Δt for $k=7$ is determined from $\nu'=3.731\times10^{-3}$, using (2.9), to be 268 s. Similarly, the maximum time step for the case filtering u, v, and h at 85° from $\nu'=1.898\times10^{-3}$ is 527 s and that for the case filtering $\delta_\lambda h$ and $\delta_\lambda u$ from $\nu'=1.909\times10^{-3}$ is 524 s.

Table 2 lists the maximum stable time step in seconds for a 5° grid with equivalent depth equal to 10^4 m as a function of longitudinal wavenumber k and various latitudes at which the prognostic variables u, v, and h are filtered. The first column is for the case of no filtering. The corresponding stable time steps resulting from filtering $\delta_\lambda h$ and $\delta_\lambda u$ would be very close to those

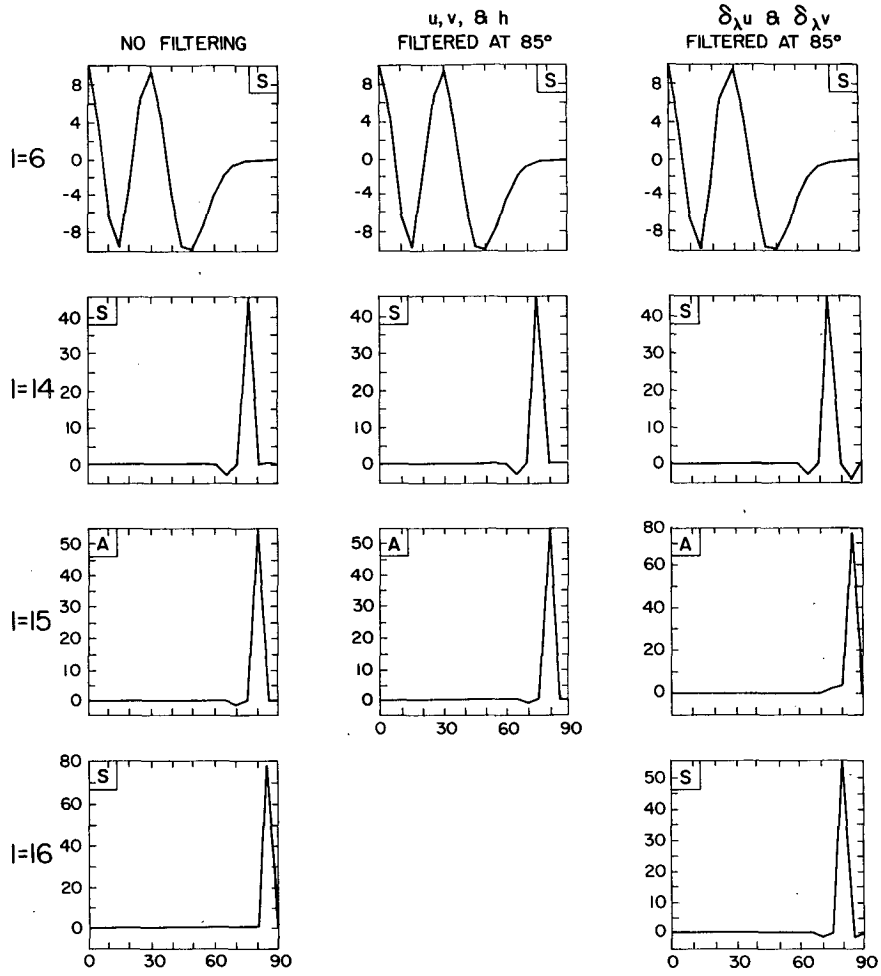

FIG. 2. Same as Fig. 1 but for Westward gravity modes with latitude indices 6, 14, 15 and 16.

resulting from filtering u, v, and h in Table 2, as indicated by Table 1.

Before discussing Table 2, we consider the number of waves at each latitude retained in a scheme that filters the prognostic variables poleward of some critical latitude so that the minimum wavelength at any latitude is greater than the wavelength at the critical latitude. Table 3 lists the number of waves retained in such a scheme as used by Williamson and Browning (1973) where the critical latitude is 60°. The modes between the horizontal lines of Table 2 indicate the stable time steps for the filtering distribution of Table 3. Wavenumbers less than 6 are not filtered, wavenumbers greater than 6 are filtered at 85°, greater than 12 at 80°, greater than 18 at 75°, etc. Once the filtering distribution is specified, the maximum stable time step can be determined from Table 2. For the waves not filtered ($k \leqslant 6$), the time step is 307 s, for those filtered at 85° but not farther equatorward ($7 \leqslant k \leqslant 12$), the time step is 353 s, for those filtered at 80° but not equatorward ($13 \leqslant k \leqslant 18$), 454 s, etc. Thus, for the scheme as a whole, the maximum stable time step is the minimum of these (307 s) to ensure that no waves are unstable.

The table shows that filtering is not needed at the lower latitudes. If wavenumbers 1 through 6 are not filtered, the maximum stable time step for these 6 waves is that of wavenumber 6, i.e., 307 s (col. 1). When the other waves, 7–36, are filtered at 85° (col. 2), the maximum time step is essentially the same, i.e., 306 s for wavenumber 18. Note that in all cases the maximum time step decreases as the wavenumber increases to wavenumber 18 (wavelength equal to $4\Delta\lambda$), then increases as the wavenumber increases to wavenumber 36 (with wavelength equal to $2\Delta\lambda$). No filtering is necessary at lower latitudes.

On the other hand, suppose it is desirable to use a 360 s time step with the 5° grid. The first column of Table 2 shows that wavenumbers 1 through 5 are stable without filtering. The second column shows that wavenumbers 6 through 11 are stable when filtered at 85° and the third column that wavenumbers 12 through 36 are stable when filtered at 80°. Filtering is not necessary at lower latitudes. Thus, the polar filtering need only be performed near the poles.

TABLE 2. Maximum stable time step (s) for 5° grid with $D=10^4$ m as a function of longitudinal wavenumber k and latitude at which the variables are first set to zero. The prognostic variables u, v, and h are filtered.

k	No filtering	Latitude 85°	80°	75°	70°	65°
2	832	1428	1665			
3	579	1080	1438			
4	444	852	1195			
5	362	703	1008			
6	307	600	871	1107		
7	268	527	769	988		
8	240	472	692	895		
9	218	430	633	821	991	
10	201	398	586	763	925	
11	188	373	550	717	872	
12	178	353	521	681	829	963
13	170	337	499	652	795	926
14	164	326	482	630	769	897
15	160	317	469	614	750	875
16	157	311	460	603	737	860
17	155	307	455	596	729	851
18	154	306	454	594	726	848
19	155	307	455	596	729	851
24	178	353	521	681	829	963
25	188	373	550	717	872	1010
30	307	600	871	1107	1295	1423
31	362	703	1008	1258	1431	1529
35	1380	1728	1751	1759	1764	1769

5. Stability on shifted mesh

The preceding analysis applies to a grid with grid points at the poles and equator. This particular distribution has the disadvantage that special codes are required for the computation at each pole. In the following, we consider a shifted grid in which the first row of grid points is $\Delta\varphi/2$ away from the pole. Likewise, grid points are $\Delta\varphi/2$ away from the equator. This grid has the advantage of needing no special approximations at the pole. We consider both second- and fourth-order approximations. The discrete equations have the same form as (2.1); the only difference is that they apply at a different set of grid points. As before, the second-order differences are given by (2.2). Fourth-order differences are

$$\left.\begin{aligned}\delta_\lambda\psi^\tau_{ij}&=\frac{4}{3}\frac{\psi^\tau_{i+1,j}-\psi^\tau_{i-1,j}}{2\Delta\lambda}-\frac{1}{3}\frac{\psi^\tau_{i+2,j}-\psi^\tau_{i-2,j}}{4\Delta\lambda}\\ \delta_\varphi\psi^\tau_{ij}&=\frac{4}{3}\frac{\psi^\tau_{i,j+1}-\psi^\tau_{i,j-1}}{2\Delta\varphi}-\frac{1}{3}\frac{\psi^\tau_{i,j+2}-\psi^\tau_{i,j-2}}{4\Delta\varphi}\end{aligned}\right\}. \quad (5.1)$$

At grid points near the poles, where the difference formulas need values across the poles, the method described in Williamson and Browning (1973) is applied, i.e., height values across the poles are used without change of sign and vector components u and v and $\cos\varphi$ across the poles are used with the sign changed. The stability analysis for the second- and fourth-order approximations on this shifted mesh has the same form as that in Section 2; only the details of the matrices are different. We present the results for the maximum stable time step here and reserve the details of the modal analysis for the Appendix.

TABLE 3. Number of waves for a 5° grid such that the minimum wavelength poleward of 60° is greater than the wavelength at 60°

Latitude	Number of waves
85	6
80	12
75	18
70	24
65	30
60	36
0	36

Tables 4 and 5 give the maximum stable time steps for various wavenumbers with no filtering and with filtering u, v, and h at various latitudes for the second- and fourth-order schemes, respectively. The low-index modes, corresponding to the large-scale Hough function solutions of the continuous shallow-water equations, are essentially the same for all methods. The high-index modes, which have the highest frequencies and thus determine the maximum stable time step, are quite different on the two grids, although the modes for the second- and fourth-order difference schemes on the shifted mesh are similar to each other.

TABLE 4. Maximum stable time step (s) for the second-order scheme on the 5° shifted mesh with $D=10^4$ m as a function of longitudinal wavenumber k and latitude at which the prognostic variables are first filtered.

k	No filtering	Latitude 87.5°	82.5°	77.5°	72.5°	67.5°
1	830	1660				
2	438	1170				
3	297	843				
4	225	654				
5	183	536				
6	155	456	739			
7	135	399	651			
8	120	357	584	796		
9	109	325	533	729		
10	101	300	493	677	846	
11	94	281	462	635	796	
12	89	266	438	602	757	898
13	85	254	419	577	725	862
14	82	245	405	557	701	835
15	80	239	394	543	683	814
16	79	234	386	533	671	800
17	78	232	382	527	664	791
18	77	231	381	525	661	789

TABLE 5. Maximum stable time step (s) for the fourth-order scheme on the 5° shifted mesh with $D=10^4$ m as a function of longitudinal wavenumber k and latitude at which the prognostic variables are first filtered.

k	No filtering	Latitude 87.5°	82.5°	77.5°	72.5°	67.5°
1	790	1275				
2	431	1060				
3	292	800				
4	220	627				
5	177	513				
6	148	432	692			
7	127	374	604			
8	112	330	536	723		
9	100	295	482	654		
10	90	268	438	598	742	
11	83	246	403	552	688	
12	77	228	374	513	642	757
13	72	213	351	482	604	715
14	68	201	331	456	572	679
15	64	191	315	434	546	650
16	62	184	303	417	525	625
17	60	178	293	404	509	606
18	58	173	286	394	497	592

To use a 360 s time step with the second-order scheme, the tables indicate that wavenumbers greater than 2 must be filtered at 87.5° and greater than 7 at 82.5°, whereas with the fourth-order scheme wavenumbers greater than 2 must be filtered at 87.5°, greater than 7 at 82.5° and greater than 12 at 77.5°. With the shifted grid, more filtering is required than with the non-shifted grid, but it is still limited to the immediate vicinity of the poles. Note that with the shifted mesh, more waves must be removed at the first row of grid points next to the pole than with the unshifted mesh for the same time step and the same finite-difference scheme. This is largely because the grid points are closer to the pole and, accordingly, the longitudinal distance between the grid points in the shifted mesh is less than that of the original mesh.

It is also interesting to compare the maximum time step allowed for the fourth-order scheme with that for the second. Gerrity *et al.* (1972) point out that the fourth-order scheme for the simple advection equation requires a time step slightly less than 0.75 the time step of the second-order scheme. Tables 4 and 5 show that this ratio also holds for the problem including gravity waves for the highest frequency waves (wavenumber 18) but not for the lower wavenumbers. For example, the corresponding ratio for wavenumber 12 is around 0.85 and for the lower wavenumbers (except wavenumber 1) is greater than 0.90. Thus, if only a few waves are retained next to the pole, the difference in maximum stable time step between second- and fourth-order approximations is relatively small.

6. Summary and discussion

We have determined the linear computational stability condition for the shallow-water equations on uniform latitude-longitude grids with and without longitudinal Fourier-filtering. Two grids are considered; the first has grid points on the equator and at the poles. The second is shifted poleward by half a grid interval so that the first row of points is half a grid interval away from the pole and no points fall on the equator or poles. On the first grid, we considered second-order differences with no filtering, with filtering the prognostic variables h, u, and v and with filtering the zonal pressure gradient ($\delta_\lambda p$) in the zonal momentum equation and the zonal divergence ($\delta_\lambda u$) in the continuity equation. On the shifted mesh, we considered both second- and fourth-order schemes with no filtering and with filtering u, v, and h. In all cases, we consider only Fourier filtering. Grid point filters with responses that are less sharp in wavenumber space have not been considered.

To allow a reasonable time step, all but approximately the longest three to six waves must be removed at the first row of points next to the pole, depending on the particular scheme. This filtering next to the pole determines a time step such that additional filtering is necessary at only a few additional latitudes, usually poleward of 75° to 80°. The time step is not increased by filtering as far south as 60° or 45°, as has been done in the past. The optimum filtering distribution depends, of course, on the time step desired and the finite-difference scheme and grid used. Elimination of unnecessary filtering saves computer time and prevents unnecessary damage to the finite-difference solutions. One potential problem that might arise from the longitudinal filtering is due to the creation of different minimum longitudinal scales at neighboring grid latitudes. This inconsistency can introduce errors in these scales into the latitudinal differences. By minimizing the region in which filtering is performed, the area in which these errors are introduced is minimized.

For a simple advection equation, Gerrity *et al.* (1972) showed that the maximum stable time step for the fourth-order approximation is slightly less than 0.75 that of the corresponding second-order scheme. Our analysis indicates that the same ratio holds for the problem including gravity waves when no filtering is performed. In general, however, when filtering is performed, the maximum stable time step is determined by the number of waves retained near the pole. For a reasonable time step, on the order of 2 to 6 waves near the poles seems desirable, depending on the particular grid. In this case, there is little difference in the maximum stable time step of the second- and fourth-order schemes.

The analysis discussed is for the shallow-water equations linearized about a state of rest and thus ignores advection. For tropospheric forecast models with an external vertical mode having an equivalent depth of around 10^4 m, the advection velocities are a fraction of the gravity wave phase speeds, especially

in the longitudinal direction near the poles where the stability condition is most critical. This analysis is a reasonable guide in choosing the particular filtering distribution for a nonlinear forecast model. We have performed many integrations with a nonlinear shallow-water model forecasting real data and with a baroclinic model making long-term simulations and forecasting real data and have found that the addition of advection does not greatly modify the stability condition. In these integrations, the prognostic variables u, v, and p were filtered every time step. Occasionally, additional filtering is necessary over that implied by the linear analysis without advection, but it generally consists of removing a few more waves at latitudes where filtering is already being performed or filtering at one additional latitude.

For example, we have made one-day forecasts from real data with a 5° baroclinic model on the shifted mesh with longitudinal filtering of the prognostic variables. The equivalent depth of the external vertical mode of this model is somewhat greater than 10^4 m. The second-order version of the model was stable with a 240 s time step when wavenumbers greater than 3 were removed at 87.5° and greater than 12 at 82.5°. The fourth-order version was stable with the 240 s time step when wavenumbers greater than 3 were removed at 87.5° and greater than 9 at 82.5°. The same model was stable with second-order differences and a 360 s time step when wavenumbers greater than 2 were removed at 87.5° and greater than 7 at 82.5°. The fourth-order version was also stable with a 360 s time step when wavenumbers greater than 2, 7 and 12 were removed at 87.5°, 82.5°, and 77.5°, respectively. We have used even longer time steps with additional filtering. For example, the second-order 5° model was stable with a 10-minute time step when wavenumbers greater than 1, 4, 7, and 10 were removed at 87.5°, 82.5°, 77.5° and 72.5°, respectively. For all these integrations, we did not try to find the maximum wavenumbers that were stable, but rather chose wavenumbers from Tables 4 and 5 somewhat within the stability range.

Acknowledgments. This study is a natural follow-up of the normal mode studies initiated by Robert Dickinson and me several years ago. I thank Bob for his continual interest and Akira Kasahara for helpful comments on the manuscript. I also thank Gerald Browning for programming assistance and Ann Lundberg for editorial assistance and typing the manuscript.

APPENDIX

Free Oscillations of Second- and Fourth-Order Model on the Shifted Mesh

Only the details of the matrices involved in the stability analysis are presented here. The analysis follows that of Section 3d of D&W and the reader is referred to that section for details of discussion omitted here.

The discrete forecast equations are given by (2.1) with the second-order difference operator defined by (2.2) or the fourth-order difference by (5.1). The discrete grid is uniform in latitude and longitude with grid points located half a grid interval away from the poles and from the equator. Values needed by the differences at points next to the poles are obtained from grid points across the poles. The sign of the scalar h is unchanged and the signs of vector components u and v and $\cos\varphi$ are changed when crossing the pole.

We assume an exponential time and longitude variation given in (2.3). Define new variables

$$\left.\begin{aligned} u_j^* &= iu_j \\ v_j^* &= v_j \\ h_j^* &= i(g/D)^{\frac{1}{2}}h_j \\ C &= (gD)^{\frac{1}{2}} \\ \sigma_j &= \cos\varphi_j \end{aligned}\right\}. \tag{A1}$$

In (A1), superscript ν and subscript k have been dropped. The solutions, determined from the equator to the pole, are divided into two classes, symmetric and antisymmetric. For the symmetric modes, u and h have the same sign in the two hemispheres and v changes sign, whereas for the antisymmetric modes u and h change sign in the two hemispheres and v has the same sign.

Define the vector of dependent variables $\mathbf{Y}$ as

$$\mathbf{Y} = \begin{bmatrix} \mathbf{Y}_1 \\ \mathbf{Y}_2 \\ \vdots \\ \mathbf{Y}_N \end{bmatrix}, \tag{A2}$$

where

$$\mathbf{Y}_j = \begin{bmatrix} u_j^* \\ v_j^* \\ h_j^* \end{bmatrix}. \tag{A3}$$

The latitudinal index j runs from 1 at the first grid point north of the equator to N at the first point south of the north pole.

The eigenvalue problem is then

$$\mathbf{LY} + \nu'\mathbf{QY} = 0, \tag{A4}$$

where

$$\mathbf{L} = \begin{bmatrix} \mathbf{A}_1\mathbf{B}_1\mathbf{D}_1 & & & & 0 \\ \mathbf{C}_2\mathbf{A}_2\mathbf{B}_2\mathbf{D}_2 & & & & \\ \mathbf{E}_3\mathbf{C}_3\mathbf{A}_3\mathbf{B}_3\mathbf{D}_3 & & & & \\ & \ddots & & & \\ & & \mathbf{E}_j\mathbf{C}_j\mathbf{A}_j\mathbf{B}_j\mathbf{D}_j & & \\ & & & \ddots & \\ & & & & \mathbf{E}_{N-2}\mathbf{C}_{N-2}\mathbf{A}_{N-2}\mathbf{B}_{N-2}\mathbf{D}_{N-2} \\ & & & & \mathbf{E}_{N-1}\mathbf{C}_{N-1}\mathbf{A}_{N-1}\mathbf{B}_{N-1} \\ 0 & & & & \mathbf{E}_N\ \mathbf{C}_N\ \mathbf{A}_N \end{bmatrix}, \tag{A5}$$

$$\mathbf{Q}=\begin{bmatrix}\mathbf{Q}_1 & & 0\\ & \ddots & \\ & & \mathbf{Q}_N\end{bmatrix}, \qquad \text{(A6)}$$

$$\mathbf{A}_j=\begin{bmatrix}0 & -\sigma_j f_j & \dfrac{k'c}{a}\\ -\sigma_j f_j & 0 & 0\\ \dfrac{k'c}{a} & 0 & 0\end{bmatrix}, \qquad \text{(A7)}$$

$$\mathbf{B}_j=\begin{bmatrix}0 & 0 & 0\\ 0 & 0 & -\dfrac{c\sigma_j}{a\Delta\varphi}\dfrac{\alpha_1}{2}\\ 0 & \dfrac{c\sigma_{j+1}}{a\Delta\varphi}\dfrac{\alpha_1}{2} & 0\end{bmatrix}, \qquad \text{(A8)}$$

$$\mathbf{C}_j=\begin{bmatrix}0 & 0 & 0\\ 0 & 0 & \dfrac{c\sigma_j}{a\Delta\varphi}\dfrac{\alpha_1}{2}\\ 0 & -\dfrac{c\sigma_{j-1}}{a\Delta\varphi}\dfrac{\alpha_1}{2} & 0\end{bmatrix}, \qquad \text{(A9)}$$

$$\mathbf{D}_j=\begin{bmatrix}0 & 0 & 0\\ 0 & 0 & \dfrac{c\sigma_j}{a\Delta\varphi}\dfrac{\alpha_2}{4}\\ 0 & -\dfrac{c\sigma_{j+2}}{a\Delta\varphi}\dfrac{\alpha_2}{4} & 0\end{bmatrix}, \qquad \text{(A10)}$$

$$\mathbf{E}_j=\begin{bmatrix}0 & 0 & 0\\ 0 & 0 & -\dfrac{c\sigma_j}{a\Delta\varphi}\dfrac{\alpha_2}{4}\\ 0 & \dfrac{c\sigma_{j-2}}{a\Delta\varphi}\dfrac{\alpha_2}{4} & 0\end{bmatrix}, \qquad \text{(A11)}$$

$$\mathbf{Q}_j=\begin{bmatrix}\sigma_j & 0 & 0\\ 0 & \sigma_j & 0\\ 0 & 0 & \sigma_j\end{bmatrix}. \qquad \text{(A12)}$$

For the second-order model, the constants α_i are given by

$$\left.\begin{aligned}\alpha_1&=1\\ \alpha_2&=0\end{aligned}\right\}, \qquad \text{(A13)}$$

and for the fourth-order model

$$\left.\begin{aligned}\alpha_1&=\tfrac{4}{3}\\ \alpha_2&=\tfrac{1}{3}\end{aligned}\right\}. \qquad \text{(A14)}$$

In general,

$$k'=\alpha_1\frac{\sin k\Delta\lambda}{\Delta\lambda}-\alpha_2\frac{\sin 2k\Delta\lambda}{2\Delta\lambda}. \qquad \text{(A15)}$$

Near the poles, the matrices are defined by

$$\mathbf{A}_N=\begin{bmatrix}0 & -\sigma_N f_N & \dfrac{ck'}{a}\\ -\sigma_N f_N & 0 & -\dfrac{c\sigma_N}{a\Delta\varphi}\dfrac{\alpha_1}{2}(-1)^k\\ \dfrac{ck'}{a} & -\dfrac{c\sigma_N}{a\Delta\varphi}\dfrac{\alpha_1}{2}(-1)^{k+1} & 0\end{bmatrix}, \qquad \text{(A16)}$$

$$\mathbf{C}_N=\begin{bmatrix}0 & 0 & 0\\ 0 & 0 & \dfrac{c\sigma_N}{a\Delta\varphi}\left[\dfrac{\alpha_1}{2}+\dfrac{\alpha_2}{4}(-1)^k\right]\\ 0 & -\dfrac{c\sigma_{N-1}}{a\Delta\varphi}\left[\dfrac{\alpha_1}{2}+\dfrac{\alpha_2}{4}(-1)^k\right] & 0\end{bmatrix}, \qquad \text{(A17)}$$

$$\mathbf{B}_{N-1}=\begin{bmatrix}0 & 0 & 0\\ 0 & 0 & -\dfrac{c\sigma_{N-1}}{a\Delta\varphi}\left[\dfrac{\alpha_1}{2}-\dfrac{\alpha_2}{4}(-1)^k\right]\\ \dfrac{c\sigma_N}{a\Delta\varphi}\left[\dfrac{\alpha_1}{2}-\dfrac{\alpha_2}{4}(-1)^{k-1}\right] & 0\end{bmatrix}. \qquad \text{(A18)}$$

At the equator, the matrices for the symmetric class are given by

$$\mathbf{A}_1=\begin{bmatrix} 0 & -\sigma_1 f_1 & \dfrac{ck'}{a} \\ -\sigma_1 f_1 & 0 & \dfrac{c\sigma_1}{a\Delta\varphi}\dfrac{\alpha_1}{2} \\ \dfrac{ck'}{a} & \dfrac{c\sigma_1}{a\Delta\varphi}\dfrac{\alpha_1}{2} & 0 \end{bmatrix}, \tag{A19}$$

$$\mathbf{B}_1=\begin{bmatrix} 0 & 0 & 0 \\ 0 & 0 & -\dfrac{c\sigma_1}{a\Delta\varphi}\left(\dfrac{\alpha_1}{4}+\dfrac{\alpha_2}{4}\right) \\ 0 & \dfrac{c\sigma_2}{a\Delta\varphi}\left(\dfrac{\alpha_1}{2}-\dfrac{\alpha_2}{4}\right) & 0 \end{bmatrix}, \tag{A20}$$

$$\mathbf{C}_2=\begin{bmatrix} 0 & 0 & 0 \\ 0 & 0 & \dfrac{c\sigma_2}{a\Delta\varphi}\left(\dfrac{\alpha_1}{2}-\dfrac{\alpha_2}{4}\right) \\ 0 & -\dfrac{c\sigma_1}{a\Delta\varphi}\left(\dfrac{\alpha_1}{2}+\dfrac{\alpha_2}{4}\right) & 0 \end{bmatrix}. \tag{A21}$$

For the antisymmetric class,

$$\mathbf{A}_1=\begin{bmatrix} 0 & -\sigma_1 f_1 & \dfrac{ck'}{a} \\ \sigma_1 f_1 & 0 & -\dfrac{c\sigma_1}{a\Delta\varphi}\dfrac{\alpha_1}{2} \\ \dfrac{ck'}{a} & -\dfrac{c\sigma_1}{a\Delta\varphi}\dfrac{\alpha_1}{2} & 0 \end{bmatrix}, \tag{A22}$$

$$\mathbf{B}_1=\begin{bmatrix} 0 & 0 & 0 \\ 0 & 0 & -\dfrac{c\sigma_1}{a\Delta\varphi}\left(\dfrac{\alpha_1}{2}-\dfrac{\alpha_2}{4}\right) \\ 0 & \dfrac{c\sigma_2}{a\Delta\varphi}\left(\dfrac{\alpha_1}{2}+\dfrac{\alpha_2}{4}\right) & 0 \end{bmatrix}, \tag{A23}$$

$$\mathbf{C}_2=\begin{bmatrix} 0 & 0 & 0 \\ 0 & 0 & \dfrac{c\sigma_2}{a\Delta\varphi}\left(\dfrac{\alpha_1}{2}+\dfrac{\alpha_2}{4}\right) \\ 0 & -\dfrac{c\sigma_1}{a\Delta\varphi}\left(\dfrac{\alpha_1}{2}-\dfrac{\alpha_2}{4}\right) & 0 \end{bmatrix}. \tag{A24}$$

The eigenvalue problem (A4) can be solved in the same way as D&W, Section 3e.

REFERENCES

Dey, C. H., 1969: A note on global forecasting with the Kurihara grid. *Mon. Wea. Rev.*, **97**, 597–601.

Dickinson, R. E., and D. L. Williamson, 1972: Free oscillations of a discrete stratified fluid with application to numerical weather prediction. *J. Atmos. Sci.*, **29**, 623–640.

Gerrity, J. P., Jr., R. D. McPherson and P. D. Polger, 1972: On the efficient reduction of truncation error in numerical weather prediction. *Mon. Wea. Rev.*, **100**, 637–643.

Holloway, J. L., Jr., M. J. Spelman and S. Manabe, 1973: Latitude-longitude grid suitable for numerical time integration of a global atmospheric model. *Mon. Wea. Rev.*, **101**, 69–78.

Kasahara, A., and W. M. Washington, 1967: NCAR global general circulation model of the atmosphere. *Mon. Wea. Rev.*, **95**, 389–402.

——, and ——, 1971: General circulation experiments with a six-layer NCAR model, including orography, cloudiness and surface temperature calculations. *J. Atmos. Sci.*, **28**, 657–701.

Kurihara, Y., 1965: Numerical integration of the primitive equations on a spherical grid. *Mon. Wea. Rev.*, **93**, 399–415.

——, and J. L. Holloway, Jr., 1967: Numerical integration of a nine-level global primitive equations model formulated by the box method. *Mon. Wea. Rev.*, **95**, 509–530.

Sankar-Rao, M., and L. Umscheid, Jr., 1969: Tests of the effect of grid resolution in a global prediction model. *Mon. Wea. Rev.*, **97**, 659–664.

Umscheid, L., Jr., and M. Sankar-Rao, 1971: Further tests of a grid system for global numerical prediction. *Mon. Wea. Rev.*, **99**, 686–690.

Vanderman, L. W., 1972: Forecasting with a global, three-layer, primitive-equation model. *Mon. Wea. Rev.*, **100**, 856–868.

Washington, W. M., and A. Kasahara, 1970: A January simulation experiment with the two-layer version of the NCAR global circulation model. *Mon. Wea. Rev.*, **98**, 559–580.

Williamson, D. L., and G. L. Browning, 1973: Comparison of grids and difference approximations for numerical weather prediction over a sphere. *J. Appl. Meteor.*, **12**, 264–274.

——, and R. E. Dickinson, 1975: Free oscillations of the NCAR global circulation model. In preparation.